Fine Particles on Mars: Observations with the Viking 1 Lander Cameras

Abstract. *Drifts of fine-grained sediment are present in the vicinity of the Viking 1 lander. Many drifts occur in the lees of large boulders. Morphologic analysis indicates that the last dynamic event was one of general deflation for at least some drifts. Particle cohesion implies that there is a distinct small-particle upturn in the threshold velocity–particle size curve; the apparent absence of the most easily moved particles (150 micrometers in diameter) may be due to their preferential transport to other regions or their preferential collisional destruction. A twilight rescan with lander cameras indicates a substantial amount of red dust with mean radius on the order of 1 micrometer in the atmosphere.*

In our previous presentation of scientific results from the Viking 1 lander cameras (*1*) we called attention to a range of aeolian phenomena, including (i) parallel arrays of fine material oriented in the lees of rocks and pointing in the same cardinal direction as large wind streaks discernible at orbital resolution, and (ii) the accumulation of drifts of fine particles to the northeast of the spacecraft. In this report we discuss in greater detail evidence for and implications of fine particles on the martian surface and in the atmosphere, based principally on new lander pictures obtained since the preparation of our previous report. Since the words "sand" and "dust" have particular particle size and even genetic implications, we describe the sediment as "fines" in this report; for similar reasons we call the accumulations of fine particles revealed by the Viking lander cameras drifts rather than dunes. Analyses of the trenches dug by the surface sampler and of material delivered to the spacecraft imply that fines, at least near the spacecraft, are largely in the size range 10 to 100 μm (*2*).

Drifts. Among the most spectacular features observed by Viking 1 lander cameras is a drift field located to the northeast of the spacecraft (Fig. 1). The drifts are associated with large boulders (2 to 3 m in dimension), suggesting that material was trapped in a region of increased surface roughness and consequent reduced wind shear stress. The boulders may also provide leeward regions of wind shadowing. In fact, two of the boulders are partially buried by fines (Fig. 2a), while a third has a cap of fine-grained material (Fig. 2b). Most of the boulders lie on the northeast side of the drifts, implying a wind direction from northeast to southwest during the depositional phase of drift formation. Note that this direction is the same as the wind direction inferred from drifts behind smaller (< 1 m) rocks and from trends of bright streaks seen from orbit (*1*). Other drift fields in the same scene also appear to be associated with large roughness elements on their northeast sides.

Topographic data derived from stereo ranging of the drifts are shown in Figs. 3 and 4. The drifts are typically only a few tens of centimeters high and a few meters wide, oriented transverse to the wind; the fine material that accumulated behind the large boulder in the farfield of Figs. 1 and 2a is several meters in height. In general, the drift field seems to have a topographic configuration that is much more irregular than terrestrial dune fields. Many of the drifts have concave surfaces and sharp edges. Interdrift areas generally reveal subjacent blocky terrain. Evidence for stratification can be seen in at least two regions. These observations imply that the last dynamic event was one of deflation rather than deposition.

The drift shown stereographically in Fig. 3 seems to be scoured in such a manner that subparallel ridges are exposed on its southwest side. The ridges run perpendicular to the inferred wind direction during deposition, which is consistent with the ridges being exposed bedding planes of a transverse drift. For this interpretation to be correct, the bedding must have been exposed along strike (its intersection with the horizontal plane) by deflation of a large portion of the southwest side of the drift. Another drift that displays stratification seems to have been scoured subparallel to the inferred wind direction (Fig. 1). This drift shows individual laminae, each estimated to be about 1 cm thick, dipping gently toward the northeast. The laminae apparently combine to form sets, a few centimeters thick, with slightly curved, generally parallel bounding surfaces. The other drift face, scoured perpendicular to the wind direction, displays horizontal dark bands with a regular spacing consistent with that of the bounding surfaces of the individual sets of laminae. The intersection of these laminae with a less steeply sloping surface oriented roughly northwest-southeast imparts a ripple-like appearance to the bedding. However, it is unlikely that these dark bands represent ripples with wavelength spacings measured in centimeters. Ripple spacing seems to be governed mainly by the characteristic skip distance traveled by saltating particles (*3*). Because of high threshold wind velocities and the low gravitational acceleration, ripple wavelengths on Mars should be much larger than on the earth, perhaps as much as many tens of meters (*4*).

Two drift fields in the middle foreground in Fig. 4 are noteworthy. They do not appear to be associated with large roughness elements and they display albedo differences. The drift at azimuth 150° (measured clockwise from north) is bright and that at 180° is dark (Fig. 4). These drifts have smooth, rounded surfaces—clearly different from the morphology of the drifts previously described. Small rocks along the southwest drift margin are partly buried by sediment, which forms a continuous drape from drift surface onto rocks.

The scoured nature of the drifts in Figs. 1 to 3 implies a change in aeolian regime from one of deposition to one of erosion. The occurrence of fines atop the large boulder in Fig. 2b may imply that fines were once partially burying the boulder in a manner similar to burial of the large block in the farfield of Fig. 1. Subsequent deflation could have removed the downwind deposits, leaving a cap of fines atop the boulder. The well-exposed laminae in the drift in Fig. 1 dip to the northeast, suggesting accretion on upwind slopes. This may indicate antidune formation, although extremely high turbulence characteristics would have had to prevail during the depositional phase. Many other features seen in the lander pictures are also consistent with deflation as the most recent dynamic event occurring at the landing site. In particular, the large rock in Fig. 2b has a textured or pitted surface, consistent with differential abrasion of mineral components with varying hardness. The abundance of bedrock outcrops (Fig. 4) also suggests removal of fines, as does the high density of blocks. Finally, linear trains of blocks radiating from a topographic high to the west of the spacecraft suggest deflation. The blocks may be dike rock that withstood abrasion and removal better than surrounding materials, exposing the dike as a series of blocks.

The timing of the change from deposition to deflation of the drifts in Fig. 1 is uncertain. The winds prevalent during deposition, as discussed, appear to be consistent with bright streak directions seen from orbit. The bright streaks presumably indicate wind directions prevalent during at least the waning phases of

Fig. 1. High-resolution view of drifts to the northeast of the spacecraft. The large boulder in the left of the picture is about 10 m from the spacecraft and about 2 m across. The meteorology boom bisects the picture. The drifts immediately to the right of the boom are shown stereographically in Fig. 3. Arrows point to regions of exposed strata, interpreted in the text as cross-bedding. This picture covers about 100° in azimuth and extends from 0° to −20° in elevation. The scene is backlit and the sun is about 27° above the horizon. Parts of the left side of the picture are viewed under different conditions of illumination in Fig. 2 (frame 11A097/014).

the yearly global dust storms. Conceivably, the drifts formed during the last storm and have been modified since then. Alternatively, the drifts could be ancient, perhaps even related to some previous epoch when the atmospheric pressure was higher. This interpretation is consistent with the proposed extremely low erosion rates that can be inferred from the distribution of ages of geologic units on Mars (*5*). In another interpretation, based on calculations predicting high abrasion rates on Mars (*6*), the region has been buried for substantial periods of time to depths of several meters or more, and only recently exhumed. The next global dust storm should begin around April 1977. Monitoring of the drift field for changes in topographic configuration and of brightness will add considerably to our knowledge of the rate of removal and redistribution of material.

Cohesion and particle velocities. A variety of observations indicate that the martian surface material has considerable cohesion. These include (i) studies of clods thrown out by the lander upon impact, (ii) the armored character of the interrock terrain, and (iii) the character of the trench dug by the sample arm. Estimates of the cohesion range as high as 10^4 dyne cm^{-2} (*2*). The presence of cohesive fines has an important impact on the efficiency of aeolian activity. Without cohesion, under martian atmospheric conditions, the value for threshold velocity would decline monotonically from large to small particle sizes, down to a particle diameter of 10 μm (*7*). The observed high cohesion implies, instead, that the curve should be roughly parabolic, with the most easily moved particles in the 100- to 200-μm range (*8*).

The preliminary conclusion (*2*) that the bulk of the fines are in the range 10 to 100 μm implies that, without an influx of particles from another region, the terrain at the landing site must be relatively stable, even during windstorms. Particles near 100 μm in diameter are near the boundary between saltation and suspension on Mars (*7*). The relative sparsity of the most readily saltating particles at the landing site implies that, without an influx from another source, recent abrasion must occur at a relatively low rate.

One explanation for the lack of particles > 100 μm may be simply that they are most readily saltated and have been transported elsewhere. Alternatively, particles of such sizes may be rapidly abraded and broken after they are introduced into the martian aeolian regime. High particle velocities, the lack of atmospheric cushioning on impact, and the possible softness of minerals involved (feldspars and pyroxenes, for example) may combine to reduce such particles rapidly to much smaller sizes by chipping and splitting.

Fines suspended in the atmosphere. Analysis of color photographs taken during the middle of the first day after landing indicates that the reflectivity of the sky at large angular distances from the sun was about twice as large in the red as in the blue (*1*). This was interpreted to indicate that red-colored particles constituted a significant fraction of the atmospheric aerosols above the landing site. Further information has now been obtained by repeatedly scanning in elevation at a constant azimuth from 20 minutes before sunset until 20 minutes after sunset.

Analysis of this "rescan" picture indicates that the sky is distinctly reddish at large elevation angles and becomes progressively less red toward the horizon. The portion of the sky close to the horizon is at a small angular distance from the sun, while the region at higher elevation angles lies at a greater angular distance from the sun in this picture. Thus, the sky becomes redder at increasing angles of scatter, θ. For example, after sunset, at a position where $\theta = 20°$, the color ratio, C, of red reflectivity to blue reflectivity equals about 1.35, while C is about 0.9 when $\theta = 2.5°$. The observation that $C > 1$ for $\theta \gtrsim 4°$ strengthens our prior argument that red-colored particles contribute significantly to the sky color. At the time the rescan was taken, the ground was much darker than the sky. Thus, reflected groundlight did not to a large extent influence the color of the sky in the twilight rescan.

The variation of C with θ permits a crude estimate of the size of the dust particles to be made. This variation in effect mirrors the competition between light that is diffracted and light that is refracted on passing through the particles. For particles larger than about 0.1 μm in radius illuminated by visible light, the diffraction cross section is nearly independent

of wavelength. Diffracted light of shorter wavelengths will be more sharply concentrated in smaller scattering angles. Thus, close to the horizon, where diffraction is the dominant mode of scattering, $C < 1$. At increasing θ, a large fraction of light is scattered by passing through the particles, so that C will increase if the particles preferentially absorb blue light. Comparison of the observed relationship between C and θ with phase functions derived from Mie scattering theory indicates that the mean particle radius has a value on the order of 1 μm. This value, which is only intended as an order of magnitude estimate, is comparable to values deduced from observations of dust particles present in the great dust storm of 1971 (*9*).

We have obtained an estimate of the extinction optical depth of the atmosphere, τ, by observing the brightness of the sun at several elevation angles. Measurements performed on the afternoon of sol 12 at elevation angles of 20° and 10° imply that $\tau \cong 0.45$ at an effective wavelength of 0.67 μm. Thus the suspended dust content of the atmosphere could form a monolayer covering a significant fraction of the surface were it to fall uniformly on the ground.

Great dust storms that sometimes shroud the entire planet are known to originate near the summer solstice in the southern hemisphere, when Mars is close to its perihelion orbital position. In addition, local dust storms occasionally take place. Thus, on time scales on the order of a martian year, very small dust particles are removed from the top layers of the martian surface; then, at a somewhat later time, they fall gently from the atmosphere and partially cover the surface. Analysis of the great dust storm of 1971 indicates that τ more or less steadily decreased from about 2 at the time Mariner 9 arrived at Mars (which was soon after the peak of the storm) to a value of only about 0.2, 3 months later (*9*). Thus it seems unlikely that enough dust storm particles could have remained suspended

Fig. 2. Views of the same region shown in Fig. 1, but with a sun elevation of 75°. The laminae to the right of the nearest drift, visible in the early morning picture (Fig. 1), are almost invisible here. The two large blocks to the left of the drifts in (a) are partly buried. The large block in (b) contains a cap of fine-grained material, occupying shallow depressions on the crest of the block (frame 11A131/022).

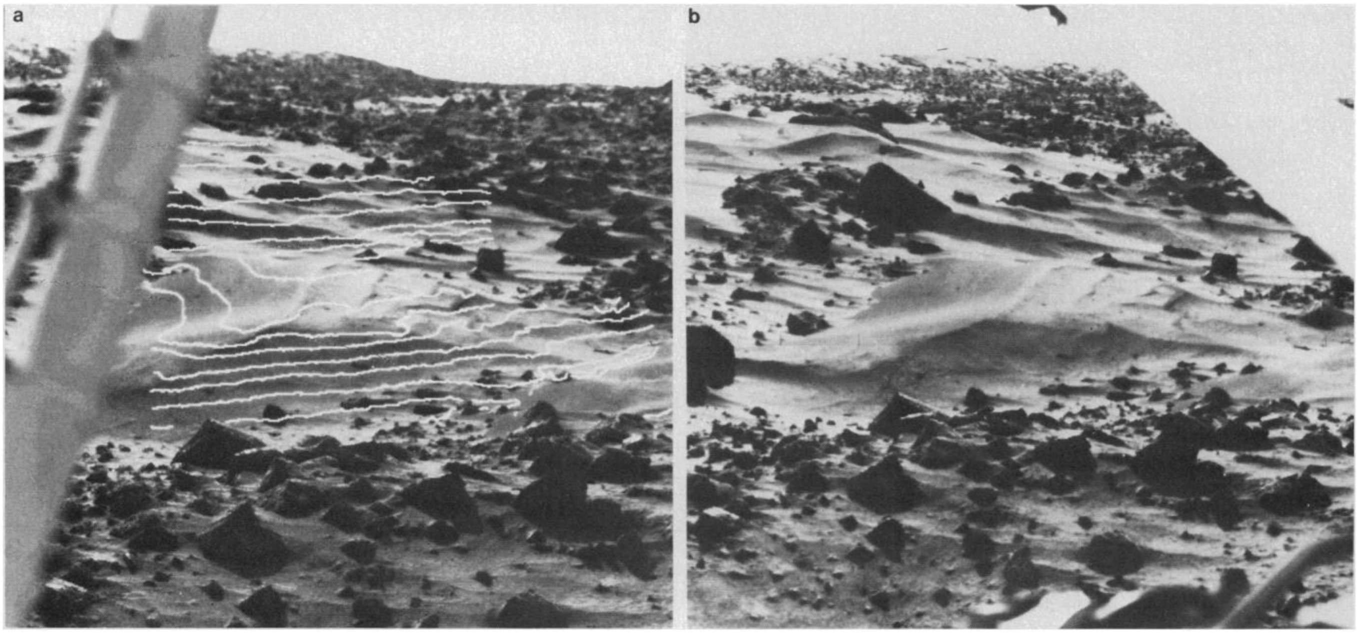

Fig. 3. Left (a) and right (b) stereoscopic views (respectively, frames 11A097/014 and 12A112/019) of the drifts shown in Fig. 1. An interactive computerized video photogrammetric system (*13*) has been used to map the drifts (for location, see Fig. 4). A selected subset of elevation contours has been overlaid by the mapping system on the left image.

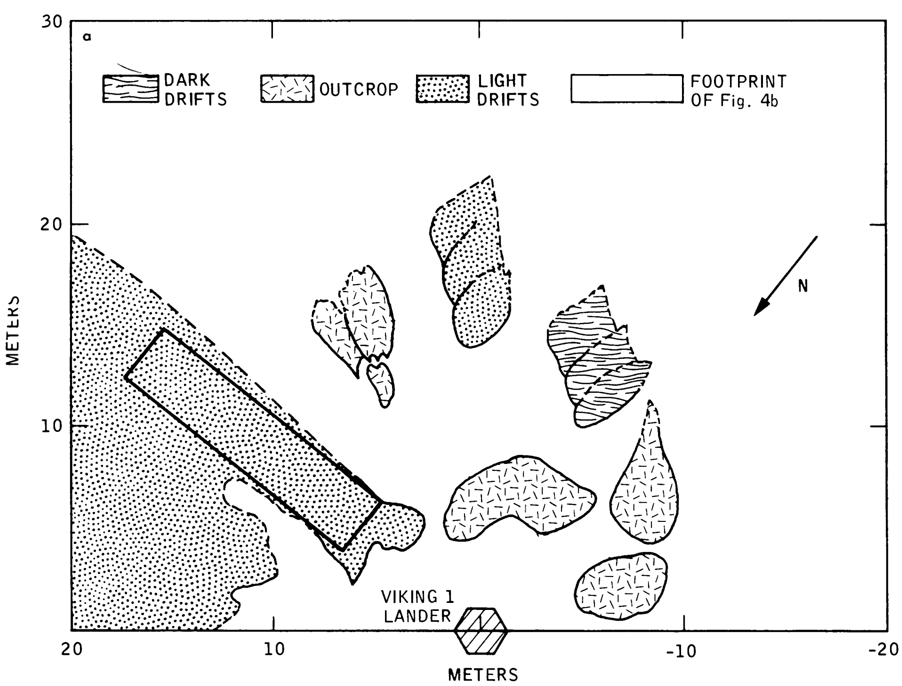

Fig. 4. (a) Planimetric sketch map derived by stereo mapping of bedrock outcrops, two regions of high- and low-albedo drifts, and the field of drifts shown in Figs. 1 to 3. Shapes of features are approximate. (b) This gravity normal elevation contour map details the inset region, by the system referenced in Fig. 3. The error bars indicate the point range uncertainty associated with camera resolution. Relative ranging accuracy finer than the point ranging uncertainty may conceivably result from the inclination of the brain to integrate over a patch of resolution elements.

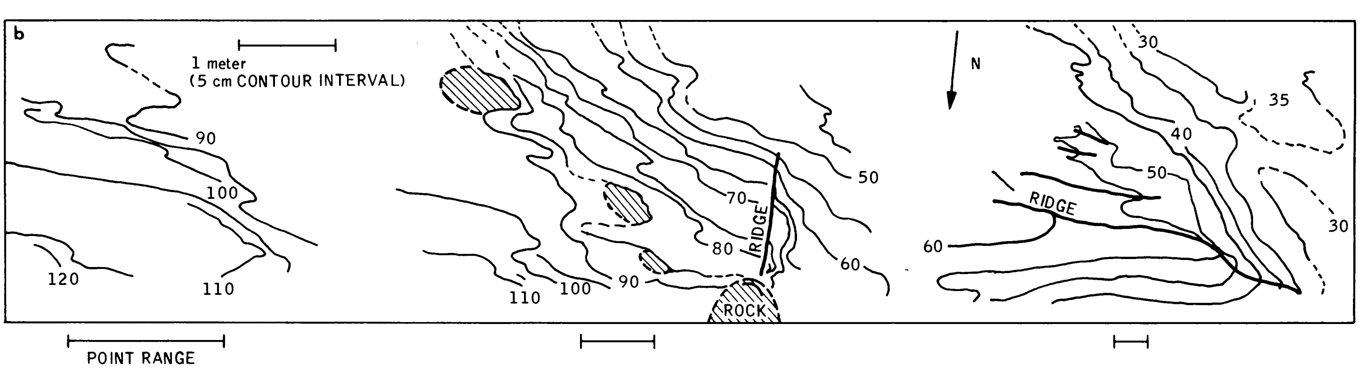

from the last southern solstice storm to cause a value of τ comparable to that found at the current epoch.

One possible source of the current suspended soil material is a hypothetical major dust storm that occurred during the previous spring season of the northern hemisphere. (Currently it is slightly past the summer solstice in the northern hemisphere.) However, earth-based polarimetric observations of Mars show no evidence for dust clouds on a planetwide scale from December 1975 to early May 1976 (*10*). Alternatively, the current optical depth could largely be due to the cumulative effect of many local dust storms during the recent past. Such a proposal is consistent with localized darkenings observed in Mariner 9 images subsequent to the decline of the great dust storm of 1971 (*11*), and with evidence for more recent localized dust storms obtained from polarization measurements of Mars made by a Franco-Soviet experiment aboard the 1974 orbiters of the Mars series (*12*).

THOMAS A. MUTCH
Department of Geological Sciences, Brown University, Providence, Rhode Island 02912
RAYMOND E. ARVIDSON
McDonnell Center for the Space Sciences, Department of Earth and Planetary Sciences, Washington University, St. Louis, Missouri 63160
ALAN B. BINDER
Institut für Geophysik, University of Kiel, Federal Republic of Germany and *Science Applications, Inc., Pasadena, California 91101*
FRIEDRICH O. HUCK
Flight Instrumentation Division, NASA Langley Research Center, Hampton, Virginia 23665
ELLIOTT C. LEVINTHAL
Department of Genetics, School of Medicine, Stanford University, Stanford, California 94305
SIDNEY LIEBES, JR.
Department of Genetics, School of Medicine, Stanford University
ELLIOT C. MORRIS
Branch of Astrogeologic Studies, U.S. Geological Survey, Flagstaff, Arizona 86001
DAG NUMMEDAL
Department of Geology, University of South Carolina, Columbia 29208
JAMES B. POLLACK
Space Science Division, NASA Ames Research Center, Moffett Field, California 94305
CARL SAGAN
Laboratory for Planetary Studies, Cornell University, Ithaca, New York 14853

1 OCTOBER 1976

References and Notes

1. T. A. Mutch, A. B. Binder, F. O. Huck, E. C. Levinthal, S. Liebes, Jr., E. C. Morris, W. R. Patterson, J. B. Pollack, C. Sagan, G. R. Taylor, *Science* **193**, 791 (1976).
2. R. W. Shorthill, H. J. Moore, II, R. F. Scott, R. E. Hutton, S. Liebes, Jr., C. R. Spitzer, *ibid.* **194**, 91 (1976).
3. R. A. Bagnold, *The Physics of Blown Sand and Desert Dunes* (Methuen, London, 1941).
4. C. Sagan, in preparation.
5. R. E. Arvidson, M. Coradini, A. Carusi, A. Coradini, M. Fulchignoni, C. Fedrico, R. Funiciello, M. Salomone, *Icarus* **27**, 503 (1976).
6. C. Sagan, *J. Geophys. Res.* **78**, 4155 (1973).
7. ——— and R. A. Bagnold, *Icarus* **26**, 209 (1975); J. B. Pollack, R. Haberle, R. Greeley, J. Iversen, *ibid.*, in press.
8. C. Sagan and J. B. Pollack, *Nature (London)* **223**, 791 (1969); R. Greeley, B. White, R. Leach, J. Iversen, J. Pollack, *Geophys. Res. Lett.* **3**, 417 (1976).
9. O. B. Toon, J. B. Pollack, C. Sagan, *Cornell University Center for Radiophysics and Space Research Report No. 639* (1976); *Icarus*, in press.
10. E. Bowell and D. Thompson, private communication.
11. C. Sagan *et al.*, *Icarus* **17**, 346 (1972); *J. Geophys. Res.* **78**, 4163 (1973); J. Veverka *et al.*, *Icarus* **21**, 317 (1974); C. Sagan *et al.*, *ibid.*, **22**, 24 (1974).
12. A. Dollfus, private communication.
13. S. Liebes, Jr., and A. A. Schwartz, in preparation.
14. We are indebted to the following members of the Viking Lander Imaging Flight Team, who have been responsible for the preparation of imaging commands sent to the lander and for the processing of returned data: P. Avrin, C. E. Carlston, E. W. Dunham, P. L. Fox, S. U. Grenander, E. A. Guinness, K. L. Jones, R. A. Kahn, W. R. Patterson, D. C. Pieri, C. W. Rowland, R. B. Tucker, G. R. Taylor, and S. D. Wall. We are also especially indebted to R. Kahn for assistance in the atmospheric analyses. This research was supported by NASA.

2 September 1976

The "Soil" of Mars (Viking 1)

Abstract. *The location of the Viking 1 lander is most ideal for the study of soil properties because it has one footpad in soft material and one on hard material. As each soil sample was acquired, information on soil properties was obtained. Although analysis is still under way, early results on bulk density, particle size, angle of internal friction, cohesion, adhesion, and penetration resistance of the soil of Mars are presented.*

Our earlier report on physical properties (*1*) covered the first 8 sols (*2*) on Mars. This report now includes data through sol 36. The landing site of the spacecraft was characterized by two physically different "soil" types (*3*), an ideal situation for measuring differences in soil properties. Footpad 2 penetrated a soft material to a substantial depth whereas footpad 3 barely penetrated at all. Figure 1 shows a sketch map of the location of these two soil types. As a result of the normal surface sampler operations to obtain "samples" (*3*) for the biology experiment, gas chromatograph–mass spectrometer experiment (GCMS), and x-ray fluorescence experiment (XRFS), soil properties experiments were carried out. Seven trenches were dug in the surface of the so-called "Sandy Flats" and the "Rocky Flats" areas. Figure 2 shows these areas before and after acquisitions were obtained. During the delivery of the soil some of the surface material fell from the collector head of the surface sampler and was blown by the surface winds, making possible an interpretation of particle size. Images of the collector head show (Fig. 3) that soil adheres to its surface after acquisition and is partially removed after exposure to vibration and winds; this allows analysis of adhesion and depth of the surface layer. After delivery to the three active soil analysis experiments, the material remaining in the collector head was purged onto the surface. Purge site images provide yet another physical properties experiment (Fig. 4). A small comminutor or grinder is included in the GCMS processing assembly; the current drawn by the comminutor motor during grinding is recorded and provides some indication of the type of material being comminuted. A complete list of the experiments used to date to obtain estimates of soil properties is given in Table 1. We present here a brief description of the immediate environs of Viking 1 and a summary of the techniques employed to deduce these properties.

Environs. The surface in the immediate vicinity of Viking 1 consists of an area with fine-grained materials (Sandy Flats), and a rocky area set in a matrix of finer-grained material (includes Rocky Flats) (Fig. 1). Fine-grained materials, which occupy 12 to 14 percent of the sample field, were deformed by small fragments and grains propelled by rocket engine exhausts (*1*) that produced small-rimmed to rimless craters and tracks aligned along radials centered on each retro-engine (Fig. 5). Footpad 2 penetrated this material, producing open fissures and both monoclinal and anticlinal flexures of the surface near the footpad (Fig. 5). Isolated open fractures also occur several meters from the footpad; these fractures may be natural or may result from the landing. The thickness of the fine-grained material increases from the mapped boundary near the early sample sites toward footpad 2. This is further shown by the depths of trenches and the penetration of footpad 2. Some